Few-Body Reactions with the Trojan Horse Method

G.G. Rapisarda[1,2,*], *R.* Spartá[3,2], and *A.* Tumino[3,2]
for ASFIN collaboration.

[1]Dipartimento di Fisica e Astronomia "Ettore Majorana," Università degli Studi di Catania, Catania I-95123, Italy
[2]Istituto Nazionale di Fisica Nucleare, Laboratori Nazionali del Sud, I-95123 Catania, Italy
[3]Facoltà di Ingegneria e Architettura, Università degli Studi "Kore", I-94100 Enna, Italy

Abstract. The Trojan Horse method (THM) is a well-established experimental technique to measure nuclear reactions of astrophysical interest avoiding the suppression of the Coulomb barrier affecting experimental direct measurements. In this paper it will describe some of the THM studies involving few-body system of interest for both nuclear physics and nuclear astrophysics, such as the sub-Coulomb proton-proton elastic scattering and the deuteron-deuteron fusion at energies of interest for primordial nucleosynthesis. Moreover, the role of the intercluster motion in nuclei used for THM measurement will be highlight for the discussed physics cases.

1 Introduction

The Trojan Horse Method (THM) (see [1–3] for recent reviews) is a well established experimental technique. Originally introduced for the study of charged-particle-induced nuclear reactions taking place in astrophysical environments, THM has been applied also to investigate the nuclear interaction in few-body systems.

THM, as other indirect methods, has been introduced to overcome the experimental problems related to the study of nuclear reactions relevant for astrophysics. Indeed, in astrophysical environments nuclear reactions take place at very low energies of the order of keV. Such energies are well below the Coulomb barrier of the interacting nuclei, being of the order of MeV. Consequently, the cross section $\sigma(E)$ drops exponentially with decreasing energy, reaching values of $10^{-9} - 10^{-12}$ barn. In these conditions the experimental evaluation of the cross section is severely hindered and in some cases even beyond present-day technical possibilities. Extrapolation from data at higher energies represents a possible solution, but the exponential decreasing of the cross section could be source of systematic uncertainties. Typically, the cross section is replaced by the astrophysical factor $S(E)$:

$$S(E) = E\sigma(E)\exp(2\pi\eta) \tag{1}$$

because of the weaker energy dependence since the Gamow factor, $\exp(2\pi\eta)$ (η is the Sommerfeld parameter), compensates for the exponential decrease of $\sigma(E)$ [4]. However, extrapolation may lead to considerable uncertainty because contributions to the cross section due to low-energy resonances or tails of broad sub-threshold resonances could be totally missed. Direct reaction measurements that succeeded to perform measurements within the energy range of astrophysical interest [5] have highlighted an enhancement of the cross section at ultra low energies due to atomic electrons surrounding the interaction nuclei referred as *electron screening* effect [6]. The enhancement factor $f_{lab}(E)$ is given by the following equation:

$$f(E)_{lab} = \frac{\sigma_s(E)}{\sigma_b(E)} \sim \exp\left[\pi\eta\left(\frac{U_e}{E}\right)\right] \tag{2}$$

where subscripts s and b indicates respectively the screened and the bare-nucleus cross section, while U_e is the electron screening potential. Since matter in stars is in the form of plasma, a different value of the enhancement factor is obtained with respect to the laboratory case, so the bare nucleus cross section $\sigma_b(E)$ is the experimental parameter required for astrophysical applications. The only way to experimentally get $\sigma_b(E)$ is still through extrapolation procedure, even when experimental data are available down to the astrophysical energy range. In this framework, many indirect methods have been developed with the aim of measuring the bare nucleus cross section for reactions of astrophysical interest, avoiding experimental problems due to Coulomb barrier and electron screening effect.

The THM has been applied in the last decades to the study of charged-particle reactions as well as neutron-induced reactions involved in several astrophysical scenarios (see [7–17] for recent results and reviews). THM has also been employed to study reaction induced by radioactive nuclei [18–21], expanding the THM research field to nuclear processes that take place in explosive astrophysical environments.

In this paper we focus on two THM applications on reactions involving few-body systems. In particular, the study of the *proton-proton* elastic scattering at sub-Coulomb energies to investigate the suppression of the Coulomb field effects, that is, the key feature that makes the THM a unique and powerful experimental approach

*e-mail: grapisarda@lns.infn.it

for the study of nuclear reactions of astrophysical interest. We report also about the study of the ^{2}H(d,p)^{3}H and ^{2}H(d,n)^{3}He channels of two-deuteron fusion process, focusing on the reaction rate evaluation [4], for astrophysical applications, and on the screening potential estimation. In the last section, the results obtained on the study of the inter-cluster motion in nuclei used for THM measurements will be briefly discussed.

2 Trojan Horse Method: basic features

THM is based on the quasi-free (QF) reaction mechanism and allows to extract the cross section of a two-body process $x+A \rightarrow b+B$, at very low center of mass (*cm*) energy performing the measurement of a suitable three-body reaction $a+A \rightarrow b+B+s$ (called Trojan Horse (TH) reaction) in the QF kinematic regime.

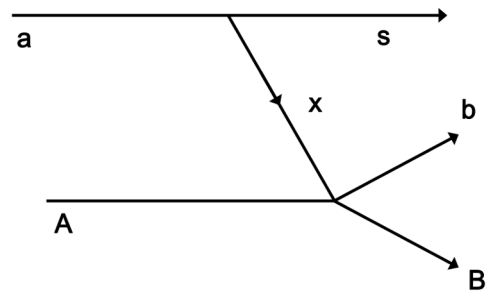

Figure 1. Polar diagram describing the TH reaction $a + A \rightarrow b + B + s$.

The nucleus a, named TH nucleus, is usually a few-body system selected for its high probability to be found in a cluster configuration $(x \oplus s)$ and acts as source of virtual projectile/target nucleus. The beam energy is fixed such that the $a + A$ interaction takes place above the $a - A$ Coulomb barrier. In this condition, the TH nucleus is subject to breakup inside the nuclear field of A and the cluster x interacts with A inducing the two-body process of interest, while the cluster s does not perturb the $x - A$ interaction, remaining *spectator* to the binary process. Figure 1 shows the polar diagram describing the TH reaction, where the three-ray vertex refers to the breakup process, while the four-ray vertex to the binary reaction. From an heuristic point of view the hypothesis of breakup within the nuclear field allows the $x - A$ interaction to take place even at zero energy without suffering the Coulomb suppression and the electron screening effect. In a more detailed description, it has to be taken into account that x is a virtual particle, that is $E_x \neq p_x^2/2m_x$. The off-energy shell nature of the $x - A$ interaction will lead to the suppression of the Coulomb field effect [1] in the binary process $x + A \rightarrow b + B$. This is the fundamental feature of the THM for astrophysical applications, moreover, this, as well be shown in sec. 3, opens new perspectives in the investigation of few-body systems interactions.

Despite the high value of the beam energy used in a TH measurament, it is possible to induce the two-body reaction at low energy down to zero. In QF conditions the two-body reaction takes place at the energy E_{QF} given by the following equation:

$$E_{QF} = \frac{m_x}{m_x + m_A} E_A - B_{xs} \tag{3}$$

where the $x-s$ binding energy B_{xs} plays a key role in compensating for the high beam energy required to overcome the $a - A$ Coulomb barrier. E_{QF} is uniquely determined from equation 3, once that the projectile energy is fixed. Actually, the QF process contribution is still high as long as the relative $x-s$ momentum p_{xs} is small compared with the bound state wave number $k_{xs} = \sqrt{2\mu_{xs}B_{xs}}$ [22]. Thus, selecting p_{xs} value within the range $0 \leq p_{xs} < k_{sx}$, it is possible to measure the two body process cross section in a wide E_{cm} range using a single beam energy. From the experimental point of view, this feature represents one of the most important advantages of the THM.

The simplest theoretical approach for THM is given by the plane-wave impulse approximation (PWIA). In PWIA the three-body cross section is factorized as in the following equation:

$$\frac{d^3\sigma}{dE_{cm}d\Omega_b d\Omega_B} \propto \mathrm{KF}|\phi(\mathbf{p}_{xs})|^2 \left(\frac{d\sigma_{xA\rightarrow bB}}{d\Omega}\right)^{HOES} \tag{4}$$

where the first term KF is the *kinematical factor*, which depends on the masses, momenta and angles of the outgoing particles [1], $|\phi(\mathbf{p}_{xs})|^2$ is the momentum distribution for the $x - s$ system given by the squared module of the Fourier transform of the radial wave function describing the $x - s$ relative motion inside a. The last factor is the differential cross section for the two-body process in the *cm* system. The *cm* energy E_{cm} is calculated following the post-collision prescription as:

$$E_{cm} = E_{bB} - Q_{2b}, \tag{5}$$

where E_{bB} is the $b - B$ relative energy and Q_{2b} is the Q-value of the binary reaction.

From equation 4 the two-body cross section can be obtained dividing the experimental three-body cross section by a Monte Carlo simulation of the $\mathrm{KF}|\phi(\mathbf{p}_{xs})|^2$ factor as shown by the following equation:

$$\left(\frac{d\sigma}{d\Omega}\right)_{bB}^{HOES} \propto \frac{d^3\sigma}{dE_{cm}d\Omega_b d\Omega_B} / \mathrm{KF}|\phi(\mathbf{p}_{xs})|^2 \tag{6}$$

The superscript *HOES* underlines that the two-body process $x + A \rightarrow b + B$ is *Half-Off-Energy-Shell*, since the entry channel is off-energy-shell due to the virtual nature of the transferred particle x. At low energies the HOES cross section reproduces the on-energy-shell (OES) one if the correction for the penetrability of the Coulomb barrier is introduced. Both experimental [23] and theoretical [24] works have demonstrated that the only consequence of the HOES nature of binary cross section consists in the suppression of the Coulomb barrier effects.

3 Proton-proton sub-Coulomb elastic scattering via THM

It is known that the $p-p$ scattering at low energy is characterized by an interference effect between the Coulomb scattering amplitude and the nuclear one [25]. In particular, the repulsive Coulomb field and the attractive nuclear one produce a destructive interference. Because of this effect, excitation function for $\vartheta_{cm} = 90°$ is characterized by a deep minimum at E_{cm} =191.2 keV (for more theoretical details refer to [25]). Several experimental measurements within the interference region confirm the theoretical expectations ([26] and references therein). The low-energy proton-proton scattering peculiarity represents an unique opportunity to further test the key THM feature, that is, the suppression of the Coulomb effect in the TH binary process. Indeed, a suppression of the Coulomb amplitude should make the interference minimum disappear and the $p-p$ excitation function should approach the $p-n$ or $n-n$ one. In this framework, $p-p$ elastic scattering around the interference minimum energy has been indirectly measured applying the THM to the three-body reaction ^{2}H(p,pp)n.

Four experimental runs [27–30] have been performed where the ^{2}H(p,pp)n reaction was induced by a proton beams of 5-6 MeV delivered on a CD_2 target, where deuteron was used as source of the virtual proton target. The two outgoing protons were detected in coincidence. The kinematic conditions of each run were changed in order to increase the QF mechanism contribution and to induce the HOES proton-proton elastic scattering at lower energy. In particular, the last two experimental runs [29, 30] allowed to fully cover the interference energy range. More experimental details can be found in [27–30].

Following the THM prescription [1], data analysis required the selection of the events corresponding to the reaction channel of interest produced by QF breakup mechanism. The contribution of the Final State Interaction (FSI) was evaluated to be less than 10% and was subtracted from experimental data [30]. Moreover, data were selected in order to have the *cm* angle ϑ_{cm} of the two-body process in the range of 90° ± 10°, where the Coulomb-nuclear interference produces the maximum effects. The experimental HOES $p-p$ scattering cross section was obtained using equation 6, by dividing the three-body coincidence yield by the factor $KF|\phi(\mathbf{p}_{xs})|^2$ obtained through a Monte Carlo calculation. $|\phi(\mathbf{p}_{xs})|^2$ was evaluated using the Fourier transform of the *s*-wave radial Hultén function for the deuteron bound state, where the expected experimental FWHM of the momentum distribution was taken into account [30, 31] (see also sec. 5). The TH $p-p$ excitation function is reported in figure 2 (black triangles) as the weighted average of the experimental data from the four THM runs.

TH data are compared with the OES $p-p$ excitation function integrated over 80° ≤ ϑ_{cm} ≤ 100° (black line in figure 2). Experimental data were normalized to the OES cross section close to the $p-p$ Coulomb barrier (500 keV). Impressively, the TH excitation function does not show any interference minimum, being in total disagreement with the OES $p-p$ one below the Coulomb barrier. On the other hand, the trends are comparable above the Coulomb barrier where the process is dominated by the nuclear field. TH data are further compared with the nucleon-nucleon nuclear $l = 0$ cross section described in terms of scattering length a and effective radius r_0. Three different calculations were performed, taking into account a and r_0 values for $p-n$, $n-n$ [32], and nuclear $p-p$ scattering [25]. Results are reported in figure 3 where the green line represents $p-n$ scattering, the red line represents $n-n$ scattering and the blue line the nuclear $p-p$ scattering. The TH cross section, within the experimental errors, is in agreement with the nucleon-nucleon nuclear cross section. This result gives a strong qualitative indication that the TH $p-p$ excitation function is dominated by the nuclear field and that the Coulomb field ef-

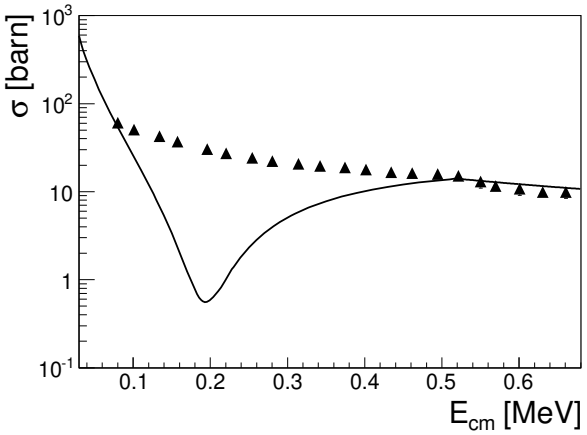

Figure 2. Black triangles represent TH $p-p$ excitation function (weighted average of the four runs) [30]. Black line is the theoretical OES $p-p$ excitation function [25].

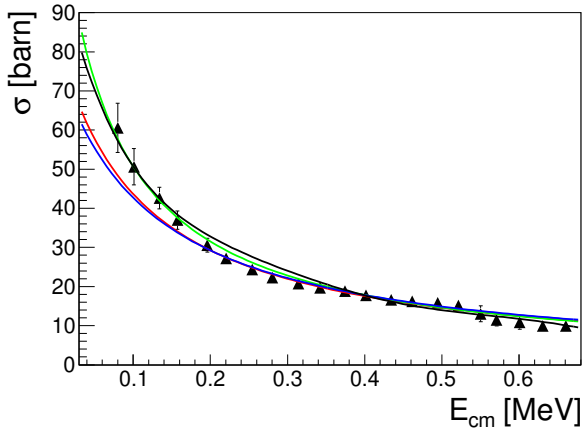

Figure 3. Black triangles represent TH $p-p$ excitation function (weighted average of the four runs). TH data are compared with low energy nucleon-nucleon cross section: green line represents $p-n$ scattering, red line represents $n-n$ scattering and the blue line the nuclear $p-p$ scattering. Black line is the theoretical HOES cross section for the low-energy $p-p$ scattering [29, 30].

fects are suppressed. TH data are further compared with an independent calculation of the theoretical low-energy $p-p$ scattering HOES cross section (black line in figure 3) [29, 30] resulting in very good agreement with the THM data. The obtained result represents a fundamental experimental test that clearly confirms the key THM feature, that is the suppression of the Coulomb effects. Moreover, it provides an interesting result from the nuclear physics point of view since, for the first time, the nuclear part of the $p-p$ interaction has been experimentally investigate at sub-Coulomb energies.

4 The *d+d* reaction studied via the THM

A great experimental effort has been devoted to the study of $p-^3$H and $n-^3$He channels of the $d+d$ reaction induced at sub-Coulomb energies, because of their crucial role for astrophysics and for applied physics. Indeed, ^{2}H(d,p)^{3}H and ^{2}H(d,n)^{3}He reactions are in the party of twelve of the Standard Big Bang Nucleosynthesis (SBBN) reactions, being strongly influential for all the primordial abundances [33], and are among the deuterium burning channels in the Pre Main Sequence (PMS) stars [4]. Besides, these reactions are among the few possible to be used in the future fusion power plants, under research at the moment [34, 35]. About the former topic, the energy range of interest spans from 0 to 1.5 MeV in order to have an accurate reaction rate calculation [4], while in the latter case the range of interest is from 0 to 30 keV.
The available data sets obtained from direct measurement show important discrepancies. Furthermore, experimental data are missing in the energy range from 200 keV and 1 MeV. Theoretical calculations deviates each other up to 15%. All these experimental and theoretical uncertainties have an important impact on the evaluation of the reaction rate. In this framework the $d+d$ interaction was studied applying the THM to get a coherent measurement of the cross sections from 30 keV to at least 1.5 MeV, to reduce the experimental errors and to obtain an accurate calculation of the reaction rates.
THM was applied to ^{2}H(^{3}He,p^{3}H)^{1}H and ^{2}H(^{3}He,n^{3}He)^{1}H three-body processes to get the astrophysical factor of the ^{2}H(d,p)^{3}H and ^{2}H(d,n)^{3}He respectively [36]. Two experimental runs were performed with a ^{3}He beam (at 17 and 18 MeV beam energy) impinging on CD_2 target (with thickness 150 μg/ cm^2). ^{3}He was used as TH nucleus for its $d \oplus p$ internal structure, as a source of virtual deuteron, while the proton is the spectator. Outgoing particles have been detected in coincidence by means of two couples of telescopes made up of two stages of silicon detectors, allowing also for particles identifications [36]. Experimental data have been analyzed using a more sophisticated theoretical approach, that made use of MPWBA [37]. The desired two-body cross sections can be considered as made of two non-resonant components for the $l = 0$ and $l = 1$ partial waves. The energy dependence of the cross section for the two components can be described by their penetrability factors [38], so that, writing the two channels $p-^3$H and $n-^3$He as $C+c$, the two-body cross section was assumed as:

$$\frac{d\sigma}{dEd\Omega}_{(d+d\rightarrow C+c)} = \frac{1}{E_{dd}} \sum_{l=0,1} C_l P_l^2 k_{dd} R T_l(k_{dd}R), \quad (7)$$

where: the relative energy E_{dd} is related to the momentum k_{dd}, to the reduced mass μ_{dd} and to the binding energy B_{dp} of ^{3}He by the relation $E_{dd} = \frac{\hbar k_{dd}^2}{2\mu_{dd}} - B_{dp}$; P_l is the Legendre polynomial; R is the channel radius; $T_l(k_{dd}R)$ is the penetrability factor [36].

To apply the MPWBA approach it is necessary to know the values of the scaling factors $C_{l=0,1}$, thus equation 7 entered in equation 6 to fit the experimental three-body coincidence yield, using C_l and the channel radius R as free parameters. The obtained values together with more details on the procedure are reported in [36].

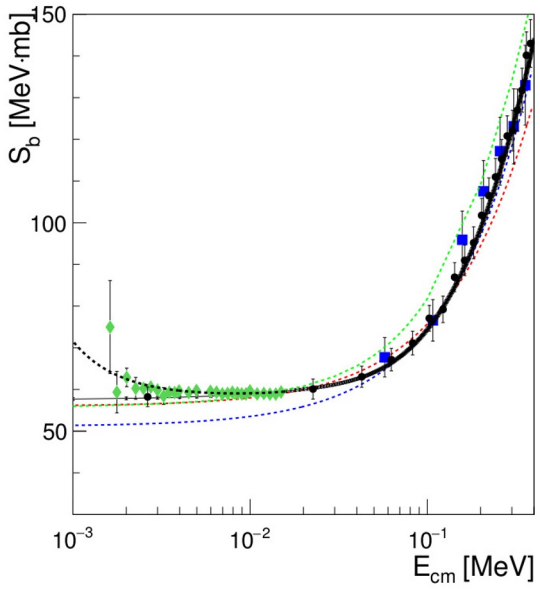

Figure 4. Bare nucleus TH S(E) for $p-^3$H channel. Black dots and blue squares represent TH data from the 18 MeV and 17 MeV runs respectively. Black solid line represents the parameterization of the THM S(E) factor (taking into account the weighted sum of two THM data sets). Low-energy data by [39] are shown as green diamonds. The black dashed line represents the result of the fit to the green diamonds. The red and blue lines are the polynomial fit by [40] and [41], while the green line is the *ab initio* calculation by [42].

Figure 4 and 5 show the bare nucleus TH S(E) factor for both $p-^3$H and $n-^3$He channels compared with low-energy data by [39], and with polynomial fits by [40] and [41] (red and blue dashed lines). In particular, black dots represent the TH astrophysical factor for both channels, obtained from the experiment with beam energy at 18 MeV. Blue squares in figure 4 represent the TH S(E) factor for $p-^3$H channel from the 17 MeV run. Moreover, the black solid lines show the parameterization of the THM S(E) factor (see [36] for details). The two-deuterons interaction is suitable for accurate *ab initio* calculation [42] shown as the green dashed line in figure 4 and 5.

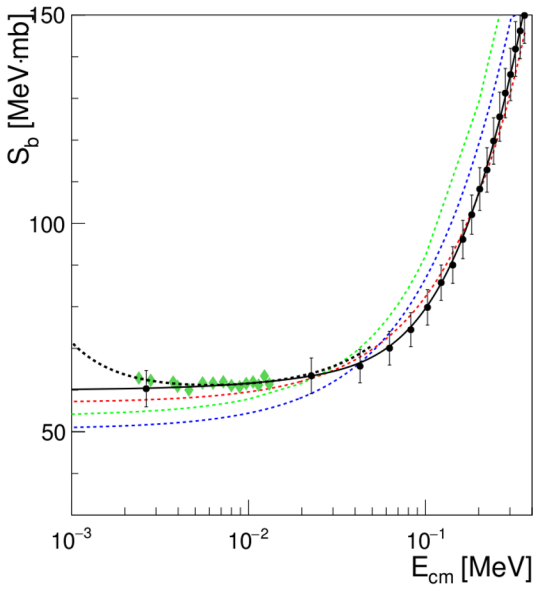

Figure 5. Bare nucleus THM S(E) for $n-^3$He channel. Black dots represent TH data. Black solid line represents the parameterization of the THM S(E) factor. Low-energy data by [39] are shown as green diamonds. The black dashed line represents the result of the fit to the green diamonds. The red and blue lines are the polynomial fit by [40] and [41], while the green line is the *ab initio* calculation by [42].

THM experiments allowed for the first time to measure the S(E) factor in a very wide energy range from 0 to 1.5 MeV. This result enabled to evaluate a very precise reaction rate, with less than 5% error, overall the region of interest for astrophysical scenarios, differing up to 20% with respect to other calculations [38, 40, 41].

Since, as mentioned before, nuclear reactions performed in the laboratory are affected by a different electron screening than in plasma, the obtained bare nucleus cross section below 30 keV provides a very important result also in the framework of study carried on the fusion power prototype plants.

Furthermore, a new estimation of the electron screening potential has been obtained. For both $p-^3$H and $n-^3$He channels, U_e has been evaluated by comparison with low energy data by Greife [39]. For the $p-^3$H channel, U_e has been evaluated in 13.4±0.6 eV, consistent with the adiabatic limit 14 eV. For $n-^3$He channel U_e =11.7±1.6 eV was evaluated, in agreement, as expected, with the result obtained for the $p-^3$H channel, but very discordant with the value given in [39] (U_e= 25±5 eV). More details about the procedure of extraction of the electron screening potential can be found in [36].

5 Study of the inter-cluster motion in nuclei used for THM measurements

A THM measurement gives access to the study of the TH nucleus inter-cluster motion. Indeed, taking into account the PWIA and the equation 4, it is possible to measure the momentum distribution of the TH nucleus. A systematic study has shown a correlation between the FWHM of the TH nucleus experimental momentum distribution and the transferred momentum from particle A to the system $F = b+B$ (see figure 1) [31]. This study considered several nuclei used as TH nucleus, here as an example the case of deuteron is discussed. In figure 6 the FWHM (indicated as W in figure and in equation 8) of the deuteron momentum distribution from different experiments (see [31] for the used data sets) is reported as a function of the transferred momentum q_t [31]. A reduction of the FWHM with respect to the theoretical value given by the Hultén function, that is 58 MeV/c, is evident at low transferred momentum. On the other hand at higher transferred momentum the FWHM approaches the theoretical value. The experimental trend have been reproduced by equation 8

$$W(q_t) = f_0[1 - \exp(-q_t/q_0)] \quad (8)$$

where f_0 = 58 MeV/c is the asymptotic theoretical value of the FWHM and q_0 = 48 ± 2 MeV/c is obtained by fitting several experimental data from literature as reported in [31]. Similar results have been obtained for the ^{3}He case as for other nuclei used in THM measurements as TH nuclei [31].

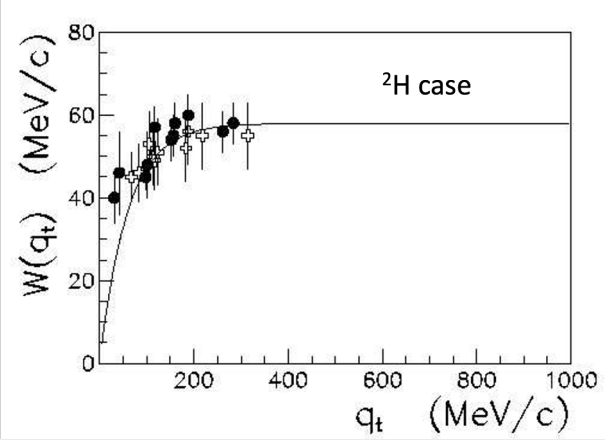

Figure 6. Deuteron experimental momentum distribution FWHM (W) as a function of the transferred momentum q_t [31].

This effect has been explain in a qualitatively way taking into account the onset of the interaction between the spectator and the final-state fragments b and B that produce a destructive interference with the pole diagram that describe the quasi-free mechanism (see figure 1). While for $q_t >> 5k_{xs}$ (with $k_{xs} = \sqrt{(2\mu B_{xs})}$ the contribution of the spectator interaction is negligible, at low energies for $q_t \approx k_{xs}$ this contribution produce a destructive interference reducing the total amplitude of the TH process. This distortion effect is reflected in the reduction of the FWHM of the momentum distribution [31]. Further theoretical analysis are required to better understand this effects. Nevertheless the applicability of the PWIA is still possible once that the experimental FWHM is taken into account.

6 Conclusions

The THM is an indirect experimental technique mainly applied for the study of nuclear reaction of astrophysical interest. On the other hand, the results described in this paper underline the possibility to apply the THM for investigation of few-body system. In particular, it has been shown how a THM measurement gives access to the nuclear part of a nuclear reaction even at sub-Coulomb energies. Further studies are ongoing in order to obtain from THM data the Coulomb free $p-p$ scattering length. Moreover, in the next future THM could be applied to the quasi-free $n+d \rightarrow n+n+p$ reaction, in order to provide a better estimation of the $n-n$ scattering length.

References

[1] C. Spitaleri, M. La Cognata, L. Lamia, R.G. Pizzone, A. Tumino, Eur. Phys. J. A **55**, 161 (2019)
[2] R.G. Pizzone et al., Eur. Phys. J. A, **56**, 283 (2020)
[3] A. Tumino, et al., Ann. Rev. Mod. Phys. **71(1)**, 345–376.(2021)
[4] C.E. Rolfs and W.S. Rodney, *Cauldrons in the Cosmos*, The University of Chicago Press, (1988)
[5] R. Bonetti, et al., Phys. Rev. Lett.**82**, 5205 (1999)
[6] H.J. Assenbaum, K. Langanke, C. Rolfs, Z. Phys. A **327**, 461 (1987)
[7] G.G. Rapisarda et al., Eur. Phys. J. A, **54**, 189, (2018)
[8] A. Cvetinovic et al., Phys. Rev. C, **97**, 065801 (2018)
[9] S. Palmerini et al., Eur. Phys. J Plus, **136**, 898 (2021)
[10] M. La Cognata et al., Astrophys. J., **941**, 96 (2022)
[11] G.L. Guardo et al., Eur. Phys. J. A, **55**, 211 (2019)
[12] R.G. Pizzone et al., Eur. Phys. J. A, **56**, 199 (2020)
[13] R. Spartá et al., Eur. Phys. J. A, **57**, 170 (2021)
[14] R. Spartá et al., Front. Astron. Space Sci., **7**, 560149, (2020)
[15] G.G. Rapisarda et al., Front. Astron. Space Sci., **7**, 589240, (2021)
[16] M.L. Sergi et al., Universe, **8**, 128 (2022)
[17] R. Spartá et al., Frontiers in Physics, **10**, 896011 (2022)
[18] R.G. Pizzone, et al., Eur. Phys. J. A, **52**, 24 (2016)
[19] M. La Cognata, et al., Astrophys. J., **846**, 65 (2017)
[20] L. Lamia, et al., Astrophys. J., **879**, 23 (2019)
[21] S. Hayakawa, et al., Astrophys. J. Lett.,**915**, L13 (2021)
[22] I.S. Shapiro, *Interaction of high-energy particles with nuclei.* International School of Physics Enrico Fermi, Course 38, edited by E.O. Ericson, p. 210, Academitices, New York (1967)
[23] M. Gulino, et al., J. Phys. G, **37**, 125105 (2010)
[24] A. M. Mukhamedzhanov, Phys. Rev. C, **84**, 044616 (2011)
[25] J. D. Jackson, J. M. Blatt, Rev. Mod. Phys.**22**, 77, (1950)
[26] H. Dombrowski, A. Khoukaz, R. Santo, Nucl. Phys. A, **619**, 97, (1997)
[27] M. Pellegriti, et al., Prog. Theor. Phys. Supp., **154**, 349, (2004)
[28] A. Tumino, et al., Nucl. Phys. A, **787**, 337, (2007)
[29] A. Tumino, et al., Phys. Rev. Lett., **98**, 252502, (2007)
[30] A. Tumino, et al., Phys. Rev. C, **78**, 064001 (2008)
[31] R.G. Pizzone, et al., Phys. Rev. C, **80**, 025807, (2009)
[32] G. A. Miller, B. M. K. Nefkens, I. Šlaus,Phys. Rep., **194**, 1, (1990)
[33] G. Steigman, **15**, 01, pp. 1-35 (2006)
[34] J. Lindl, Physics of Plasmas **2**, 3933 (1995)
[35] C. Yamanaka, *Inertial confinement fusion: The quest for ignition and energy gain using indirect drive*,, Nuclear Fusion, **39**, 6 (1999)
[36] A. Tumino et al., Astrophys. J.**785**, 96, (2014)
[37] S. Typel and G. Baur, AnPhy **203**, 228 (2003)
[38] P. Descouvemont et al., ADNDT **88**, 203 (2004)
[39] U. Greife et al., Z. Phys. A **351**, 107-112 (1995)
[40] C. Angulo et al., Nucl. Phys. A**656**, 3-183 (1999)
[41] R. H. Cyburt, Phys. Rev. D **70**, 023505 (2004)
[42] K. Arai et al., Phys. Rev. Letters **107**, 132502 (2011)